Microstructure and Mechanical Properties of Austenitic Stainless Steels After Cold Rolling

M. Hadji and R. Badji

(Submitted 23 July 2001; in revised form 12 December 2001)

The effect of austenite stability on the evolution of microstructure and mechanical properties of three austenitic stainless steels during cold rolling has been studied. Samples of different grain sizes have been used to characterize the microstructures during deformation. In the case of 304/8% Ni and 304/10% Ni stainless steels, the transformation microstructures consist of mechanical twins: ϵ-martensite and α′-martensite. No hexagonal close-packed (hcp) ϵ-martensite was detected in 316 stainless steel. The volume fraction of α′-martensite formed increases with increasing strain in 304 and 316 stainless steels for a given grain size. The amount of α′ phase increases with a decrease in grain size in 304 stainless steel, while the formation of this phase has been found to be grain size insensitive in 316 stainless steel. The strain-hardening behavior exhibited by the three stainless steels used in this study indicates the contribution of both α′-martensite and grain size strengthening in the case of both 304 stainless steels, while only grain size contribution was found in the case of 316 stainless steel.

Keywords deformation twinning, slip, stacking fault energy, strain-induced martensite

1. Introduction

Deformation-induced martensite (DIM) may be classified under two categories: stress-assisted and strain-induced. Stress-assisted martensite (SAM), with body-centered cubic (bcc) crystal structure, is formed during deformation when the stress levels simply provide for the reduction in the driving force required for the transformation from austenite to martensite.[1] The type of martensite obtained in this case is similar to that obtained by thermal quenching of austenite. However, strain-induced martensite (SIM) is a direct consequence of the plastic deformation of the austenite and can be morphologically different from stress-assisted or thermally produced martensite.[1,2]

The strain-induced martensite (α′) forms by plastic deformation of the parent austenite, where the proper defect structure is created and acts as an embryo for the transformation product. The potential nucleation sites for these embryos may include deformation twins, stacking faults, and hcp martensites.[3-5] Stacking fault energy (SFE) of austenite, as a function of alloy composition and temperature, is one of the important factors that control the characteristics of deformation mechanism during deformation. As SFE increases, the dominant deformation mode is shifted from ϵ-martensite formation to deformation twinning and then to slip.[6] Several investigators showed conclusively that ϵ-martensite is formed directly from the γ phase and that it can act as an intermediate transformation product. However, the formation of α′-martensite has been quite conclusively shown to be independent of ϵ-martensite by several authors.[5-7]

M. Hadji and **R. Badji,** Institute of Mechanical Engineering, Department of Materials Science and Engineering, University of Blida, P.O. Box 270, Blida, Algeria. Contact e-mail: hadji_n@yahoo.com.

The purpose of the current study is to elucidate the effect of nickel content on the phase transformation of Cr-Ni austenitic stainless steels with respect to the formation of deformation-induced martensite. In addition, the relationship between the change in microstructure and austenite stability with respect to α′ formation is also investigated.

2. Experimental Procedures

The chemical composition of the stainless steels used in this study is given in Table I. Besides the nickel and molybdenum contents, the chemical composition of the three stainless steels can be considered to be similar.

The as-received steels were in the annealed condition with initial grain sizes of 15, 27, and 18 μm, respectively. In order to get different grain sizes in each steel, an isochronal annealing for 1 h at temperatures in the range 1000–1200 °C were performed on samples of each stainless steel. The as-received and annealed samples were subjected to rolling to achieve 16%, 30%, 40%, and 50% reduction in thickness. Standard techniques of mechanical polishing were employed to prepare the samples for optical microscopy. X-ray diffraction method was used to identify the phases formed during deformation and to calculate the volume fraction of α′-martensite after each percentage reduction in thickness. Tensile tests and Vickers hardness were done on deformed samples in order to illustrate the mechanical behavior of these steels.

3. Results and Discussion

3.1 Microstructural Evolution During Room-Temperature Rolling

Figure 1(a) shows the microstructure of 304/8% Ni deformed at 16% reduction in thickness. The figure shows clearly the presence of shear bands and their intersections. Staudham-

mer and colleagues[5] have showed that these microshear band intersections are stacking fault free-energy dependent as well as temperature- and strain rate-dependent, and that the number of these intersections increases with decreasing SFE. With increasing strain, the number of these shear band intersections increases, leading to the nucleation of strain-induced martensite. Figure 1(b) shows the microstructure of 304/8% Ni rolled at 50% reduction in thickness. Here, in contrast with Fig. 1(a), the shear intersections and mechanical twins are difficult to resolve. Figures 2(a) and (b) show the microstructures of 304/10% Ni samples rolled at 16% and 50% reduction in thickness, respectively. The steel shows similar microstructural changes to those observed in 304/8. We note that the number of shear band and mechanical twin intersections after each strain rate is less than that observed in the case of 304/8. This is due to the fact that an increase in nickel content (from 8.6% to 10.6%)

Table 1 Chemical Compositions of Austenitic Stainless Steels Used in This Study (in wt.%)

Steel	C	Si	Mn	P	Cr	Mo	Ni	Co	Cu	Fe
Z6CN18-8 (304/8)	0.052	0.52	0.974	0.027	19.01	0.222	8.60	0.196	0.176	Balance
Z6CN18-10 (304/10)	0.049	0.40	0.974	0.025	18.53	0.180	10.4	0.197	0.080	Balance
Z6CND17-12 (316)	0.050	0.39	0.330	0.034	17.18	2.520	12.7	0.199	0.322	Balance

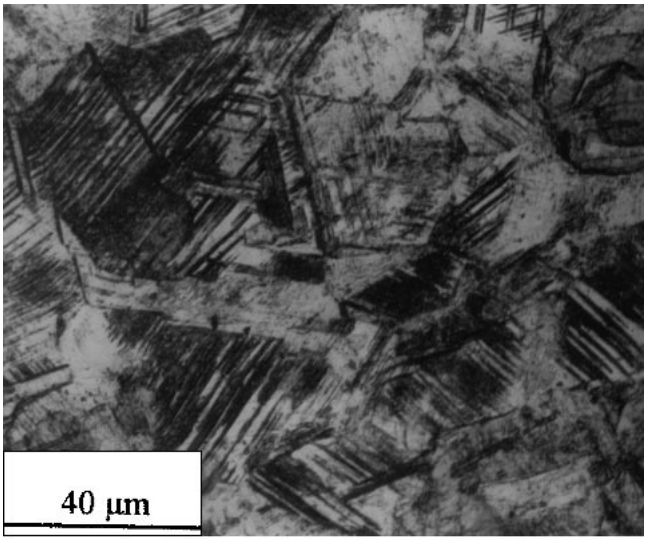

Fig. 1 Optical micrographs of 304/8% Ni rolled at **(a)** 16% and **(b)** 50% reduction in thickness

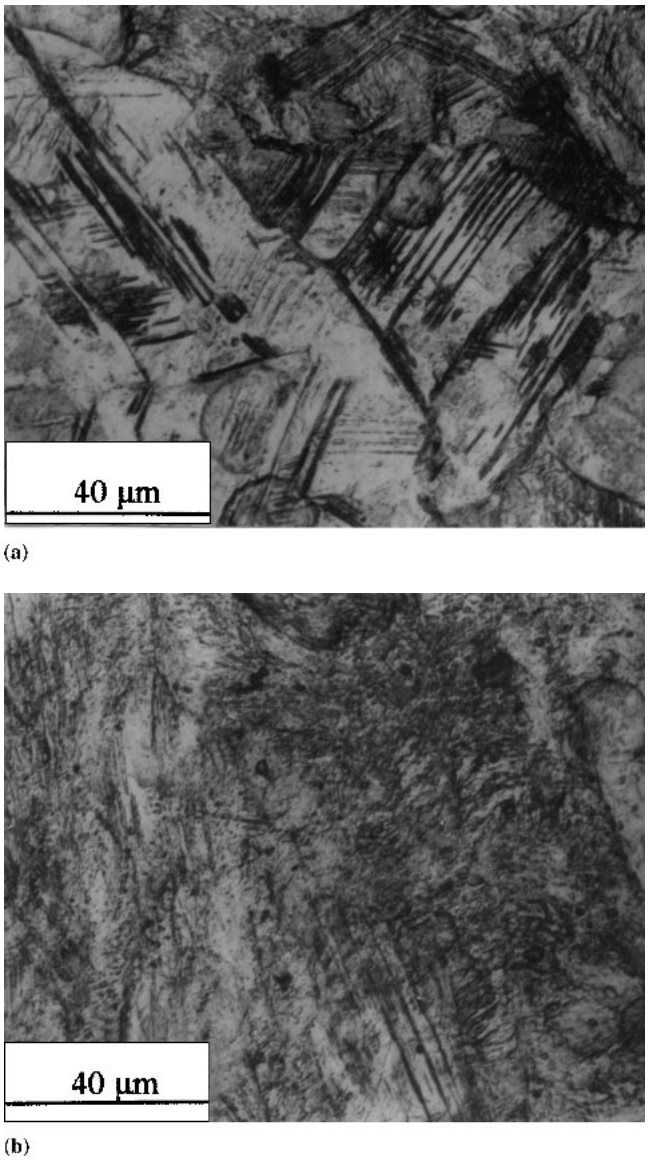

Fig. 2 Optical micrographs of 304/10% Ni rolled at **(a)** 16% and **(b)** 50% reduction in thickness

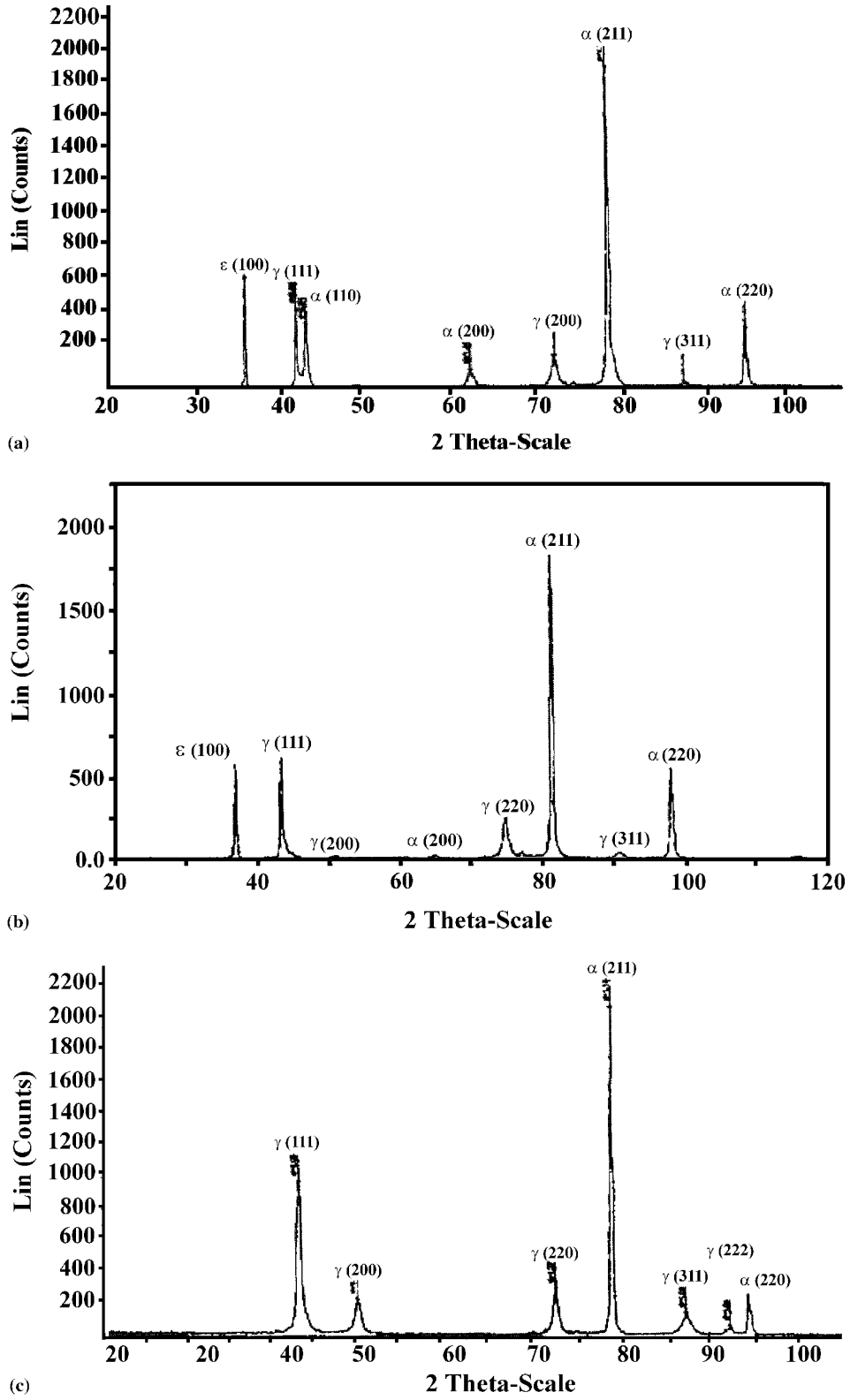

Fig. 3 XRD results at 50% reduction in thickness: **(a)** 304/8% Ni, **(b)** 304/10% Ni, **(c)** 316 stainless steel

leads to an increase in austenite stability, which makes the steel less sensitive to plastic deformation. The strain-induced martensite formed during deformation of the three stainless steels used in this study was detected by using x-ray diffraction (XRD) techniques. The results of XRD analysis conducted on 304/8% Ni and 304/10% Ni is represented in Fig. 3(a) and (b),

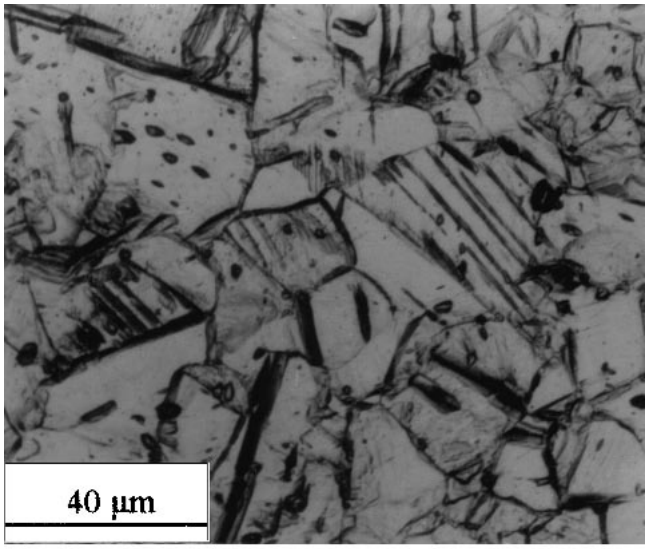

(a)

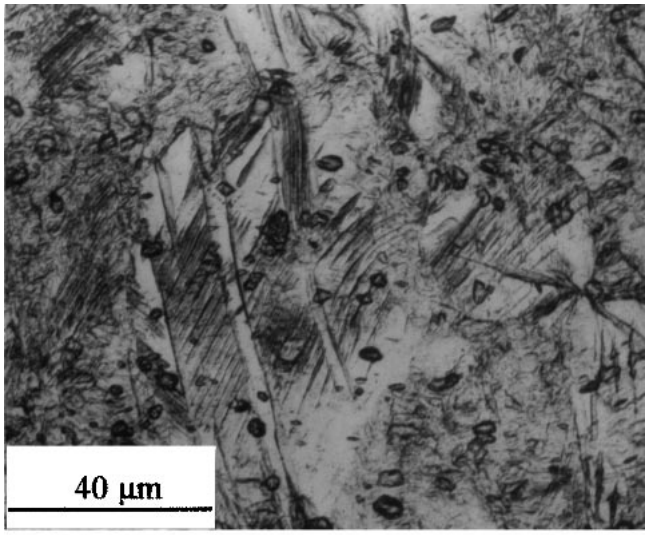

(b)

Fig. 4 Optical micrographs of 316 rolled at **(a)** 16% and **(b)** 50% reduction in thickness

respectively. The formation of α', characterized by $(110)_{\alpha'}$, $(200)_{\alpha'}$, $(211)_{\alpha'}$, and $(220)_{\alpha'}$ peaks, was detected at a strain of 16%. In addition to α'-martensite, ϵ-martensite characterized by $(100)_{\epsilon}$ peak was also detected during deformation. Hecker et al.[5] and McDowell et al.[7] have shown that the formation of ϵ-martensite during deformation of type 304 stainless steel is promoted by the low stacking fault energy of the austenite matrix and the easy shift of atoms to an hcp structure. Figure 4(a) shows the microstructure of type 316 stainless steel rolled at 16% reduction in thickness. A comparison of this figure with the features presented in Fig. 1 and 2 shows that only some parallel mechanical twins and shear bands are observed and no α' nucleation was detected at this strain. On increasing deformation to 50% reduction in thickness, the number of shear bands and mechanical twins increases. Figure 3(c) shows the results of XRD analysis conducted on deformed samples of 316

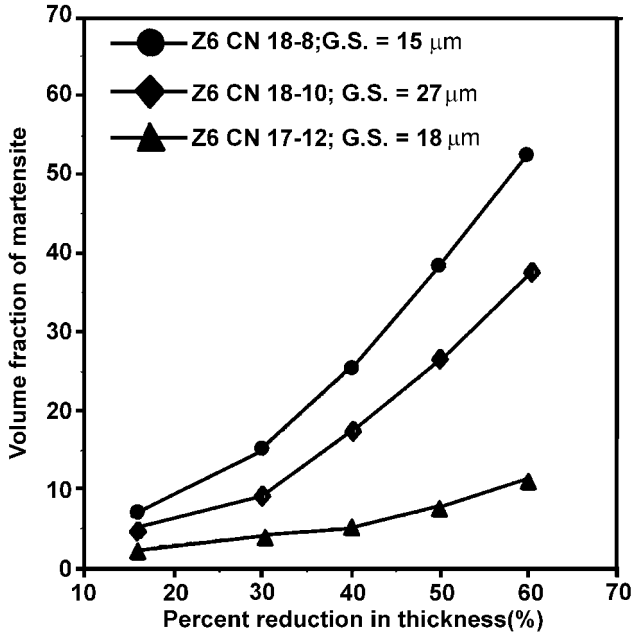

Fig. 5 Volume fraction of martensite vs reduction in thickness (for 3 stainless steels)

stainless steel. Here, contrary to 304 stainless steel, only α' peaks were detected and no ϵ-martensite was observed in this stainless steel. The absence of ϵ-martensite formation during cold rolling of 316 stainless steel indicates that the deformation mode follows the sequence of $\gamma \rightarrow$ mechanical twinning $\rightarrow$ α'-martensite rather than the sequence of $\gamma \rightarrow \epsilon$-martensite $\rightarrow$ α'-martensite.

Figure 5 shows the variation of the amount of α'-martensite versus percent reduction in thickness for the three stainless steels. The figure shows that the volume fraction of α'-martensite increases with increasing strain in both 304/8% Ni and 304/10% Ni, whereas a slight increment in the amount of SIM with deformation was observed in the case of 316 stainless steel. The figure shows also that for a fixed percentage reduction thickness, the amount of α'-martensite is always higher in 304 stainless steel than in 316 stainless steel. The lower amounts of SIM obtained in 316 in comparison to 304 stainless steel are attributed to the high stability of the γ phase, which is due to its nickel content (12.75% Ni). Figures 6-8 show the variations of the volume fraction of α'-martensite versus percentage reduction in thickness for different grain sizes for the three stainless steels, respectively. In Fig. 6 and 7, the amount of α' increases with increasing strain. In addition, the figures shows a grain size dependence of DIM; the amount of α' is more important for the smallest grain diameter after each percentage reduction in thickness. The grain size dependence of α'-martensite can be attributed to the fact that grain boundaries are preferred nucleation sites for α' phase, and that the increase in grain diameter leads to the suppression of a considerable number of nucleation sites. The behavior presented by 316 stainless steel in Fig. 8 is different from that presented by 304 stainless steel. Here, contrary to the case of 304 stainless steel, the formation of α'-martensite appears to be grain size insensitive at least for the grain diameter values used in this study.

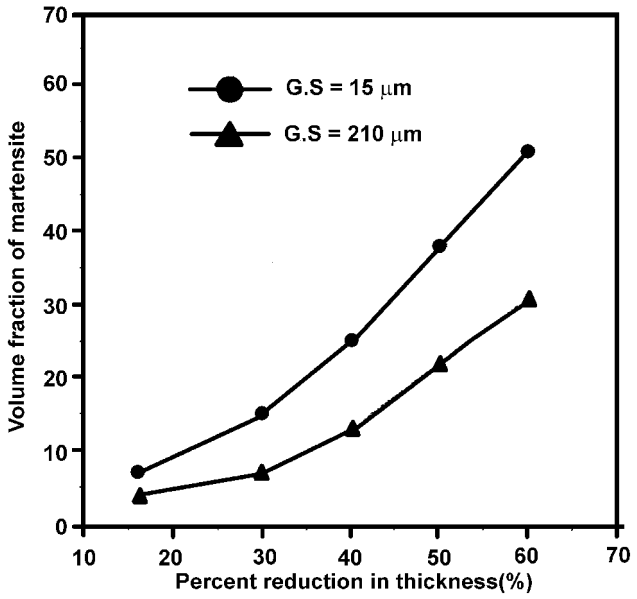

Fig. 6 Volume fraction of martensite vs reduction in thickness 304/8 stainless steel

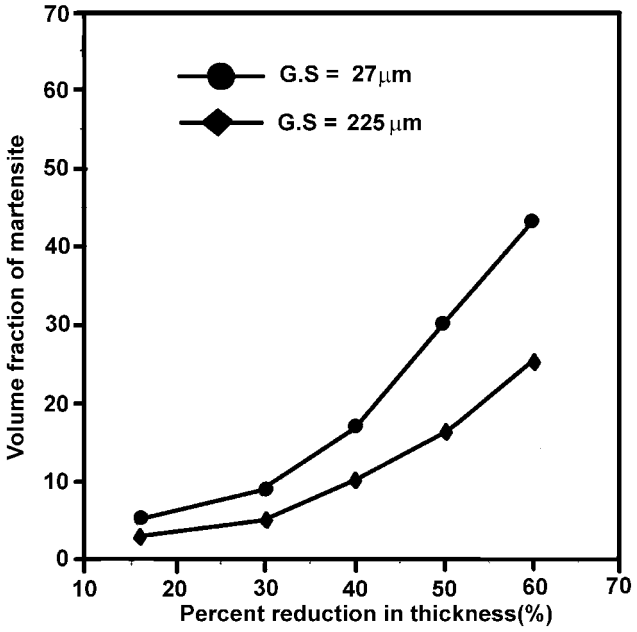

Fig. 7 Volume fraction of martensite vs reduction in thickness, 304/10 stainless steel

The role of grain boundaries in the formation of deformation-induced martensite may be explained on the basis of the stacking faults energy (SFE) value of 316 stainless steel (42 mJ/m^2) relative to that of 304 stainless steel (21 mJ/m^2).[4,6,8] The lower SFE value for 304 stainless steel will obviously result in more planar slip compared to the easier cross-slip, which is to be expected in 316 stainless steel. This would indicate the larger number of shear band intersections per unit area in the case of 304 compared with 316 stainless steel.

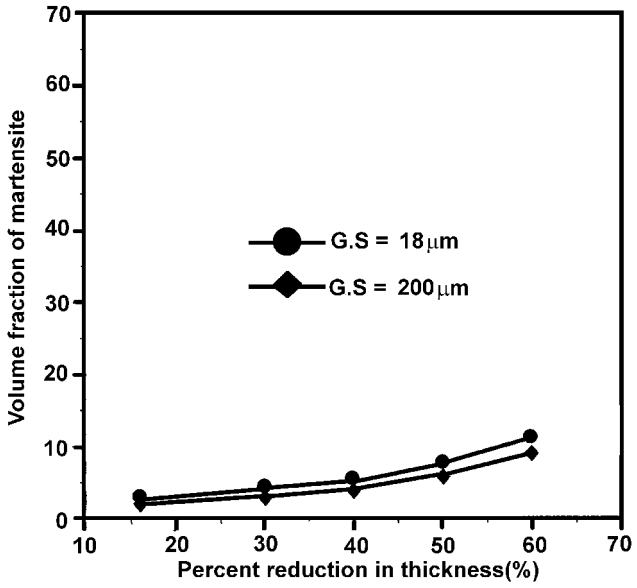

Fig. 8 Volume fraction of martensite vs reduction in thickness, 316 stainless steel

3.2 Mechanical Behavior

The mechanical properties of austenitic stainless steels are strongly affected by the martensitic transformation induced during deformation. Figures 9-11 show the variation of Vickers hardness as a function of percentage reduction in thickness for different grain sizes in the three stainless steels, respectively. It can be seen from these figures that the increase in hardness values in both 304 stainless steels is stronger than that in the case of 316 stainless steel. The lower hardness values obtained in 316 in comparison to 304 stainless steel is attributed to the high volume fraction of α'-martensite in the 304 stainless steel. The figures also show the hardness values to increase with a decrease in grain size. Figure 12 shows the variation of flow stress versus percentage reduction in thickness for the three stainless steels. The figure explains clearly the strain-hardening phenomenon that occurred in 304/8% Ni in comparison to 304/10% Ni and 316 stainless steel. The hardening phenomenon can be explained on the basis of two important factors. First, strain hardening is attributed to the decrease in austenitic grain size under the effect of deformation, which leads to an increase in grain density and hence to an increase in number of grain boundaries. This effect of grain boundaries plays an important role, as these are considered as crystalline defects, which disturb dislocation movement. As a result, a high dislocation density will be obtained in deformed stainless steels. Second, the strain-hardening phenomenon can also be attributed to the formation of deformation-induced martensite. The difference in flow stress and hardness values between the three stainless steels after each percentage reduction in thickness is due to the amount of SIM obtained in each steel at this strain. The lower values of SIM obtained in 316 stainless steel in comparison to those obtained in 304 stainless steel leads to the conclusion that the contribution of α'-martensite to the strengthening phenomenon of 316 stainless steel is neglected in comparison to the grain size contribution.

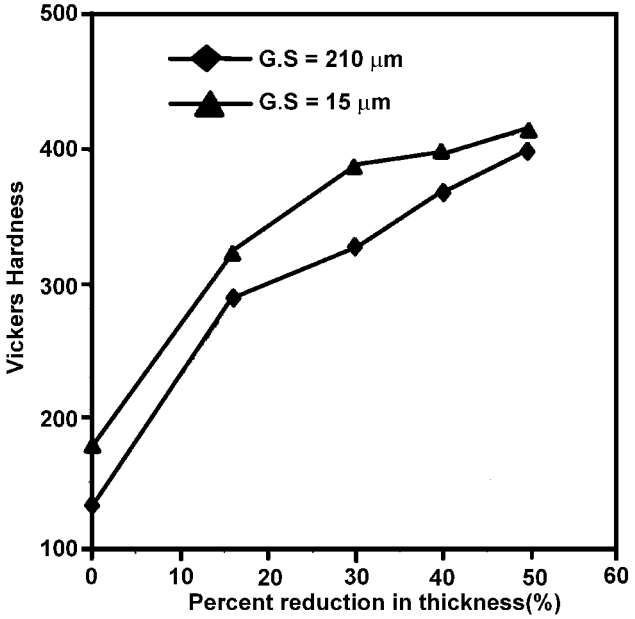

Fig. 9 Vickers hardness vs percentage in thickness, 304/8% Ni

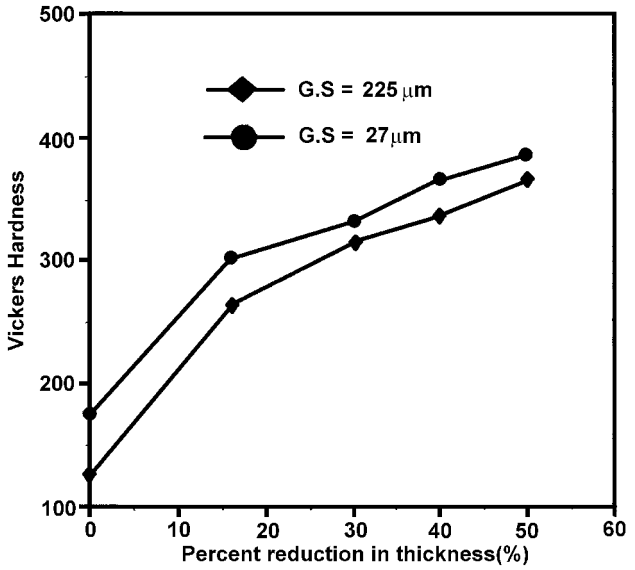

Fig. 10 Vickers hardness vs percentage in thickness, 304 10% Ni

4. Conclusions

From the observations and the experimental data obtained, the following are the key observations.

1) The deformation mechanism is closely related to the stacking fault energy of austenite. For lower SFE values (the case of 304 stainless steel), a mixture of ϵ-martensite and mechanical twins appear as intermediate phases before the formation of α′. On increasing SFE values (the case of 316 stainless steel), mechanical twinning becomes the most dominant deformation mode, and no ϵ-martensite was detected in this steel.

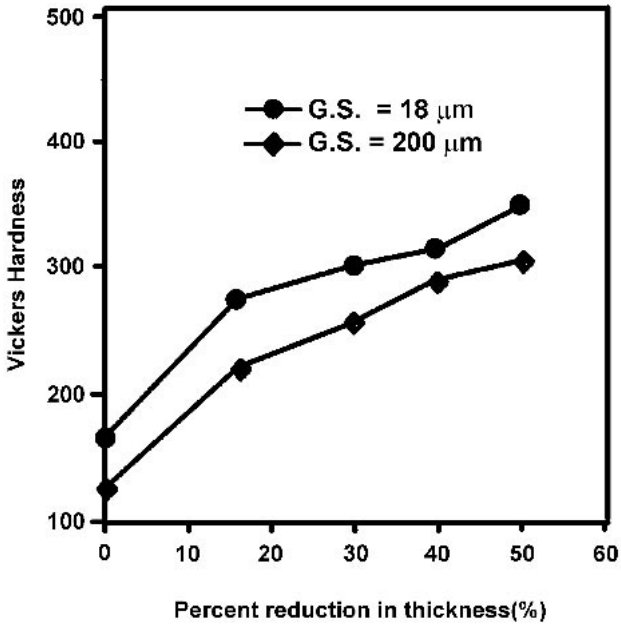

Fig. 11 Vickers hardness vs percentage in thickness, 316 stainless steel

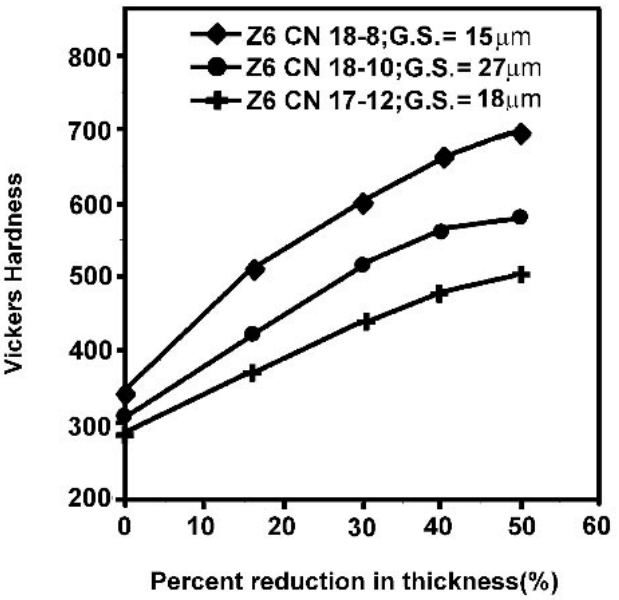

Fig. 12 Flow stress vs percentage in thickness for 3 stainless steels

2) The volume fraction of SIM formed during deformation in the three stainless steels used in this study has the following characteristics: it increases with strain in both 304 and 316 stainless steels; it is grain size sensitive in 304 stainless steel and increases with a decrease in grain size; and it is grain size insensitive in 316 stainless steel.
3) The strain-hardening behavior exhibited by the three stainless steels used in this study indicates the contribution of both α′-martensite and grain size strengthening in the case

of both 304 stainless steels, while only grain size contribution was found in the case of 316 stainless steel.

References

1. T. Narutani: "Effect of Deformation-Induced Martensite Transformation on the Plastic Behavior of Metastable Austenitic Stainless Steel," *Mater. Trans.*, 1989, *30*, p. 33.
2. S.K. Varma, J. Kalyanam, L.E. Murr, and V. Srinivas: "Effect of Grain Size on Deformation-Induced Martensite Formation in 304 and 316 Stainless Steels During Room Temperature Tensile Testing," *J. Mater. Sci. Lett.*, 1994, *13*, p. 107.
3. X.F. Fang and W. Dahl: "Strain Hardening and Transformation Mechanism of Deformation-Induced Martensite Transformation in Metastable Austenitic Stainless Steels," *Mater. Sci. Eng. A*, 1991, *141*, p. 189.
4. A.H. Advani, L.E. Murr, D.J. Matlock, and R.J. Romero: "Deformation-Induced Microstructure and Martensite Effects on Transgranular Carbide Precipitation in Type 304 Stainless Steels," *Acta Metall.*, 1993, *41*, p. 267.
5. K.P. Staudhammer, L.E. Murr, and S.S. Hecker: "Nucleation and Evolution of Strain-Induced Martensite Embryos and Substructure in Stainless Steel: A Transmission Electron Microscopy Study," *Acta Metall.*, 1983, *31*, p. 267.
6. J.Y. Choi and W. Jin: "Strain-Induced Martensite Formation and Its Effect on Strain Hardening Behavior in the Cold-Drawn 304 Austenitic Stainless Steels," *Scr. Mater.*, 1997, *36*, p. 99.
7. D.L. McDowell, D.R. Stahl, S.R. Stock, and S.D. Antolovich: "Biaxal Path Dependence of Deformation Substructure of Type 304 Stainless Steel," *Metall. Trans. A*, 1988, *9*, p. 1277.
8. B.W. Oh, S.J. Cho, Y.G. Kin, Y.P. Kin, W.S. Kin, and S.H. Hong: "Deformation Microstructures and the Shear Strain Rate of Type 304 Stainless Steel in Cylindrical Deep D of Warm Working," *Mater. Sci. Eng. A*, 1995, *197*, p. 147.